

INTERACTION OF LASER RADIATION WITH MATTER. LASER PLASMA

PACS numbers: 52.25.Tx; 52.50.Jm
DOI: 10.1070/QE2004v034n06ABEH002767

Effect of the electronic structure of target atoms on the emission continuum of laser plasma

N.E. Kask, S.V. Michurin, G.M. Fedorov

Abstract. **The low-temperature laser plasma at the surface of metal targets is experimentally investigated. Continuous spectra emitted from a laser plume are found to be similar for targets consisting of the elements of the same subgroup of the Mendeleev periodic table. The similarity manifests itself both in the dependence of the emission intensity on the external pressure and in the structure of absorption bands related to a fine-dispersed phase existing in the peripheral regions of the plume.**

Keywords: *laser plume, cluster plasma, optical spectra.*

1. Introduction

The relation between the characteristics of optical breakdown plasmas (laser plasmas) and the electronic structure of target atoms was first pointed out in paper [1], where the variation in the plasma ejection regime upon exceeding some threshold intensity was studied and the law of the variation in this threshold for metals located consecutively in the Mendeleev periodic table was found. In Ref. [1], CO_2-laser radiation with an intensity of 10^9 W cm^{-2} was used and the electron – ion plasma with a rather high temperature ($\sim 10^5$ K) was produced.

It remains to elucidate the question of the effect of the electronic structure of target atoms on the characteristics of the low-temperature laser plasma, where fine-dispersed particles, including molecular associates and gas-like clusters, begin to play a significant role [2]. Many characteristics of microscopic structures and macroobjects are known to depend on the electronic structure. For instance, the atomic radius, the ionisation potential, the melting temperature, the latent heat of vaporisation, the electric conduction, the work function, and other parameters of metals depend on the number of the group of the periodic table, varying only slightly within the group and exhibiting a significant change in going from one group to another.

In a low-temperature laser plasma, the contribution of condensate nanoparticles (clusters) to the radiation with a continuous spectrum quite often is dominant [3, 4]. The emission of clusters is well approximated by blackbody radiation spectrum with an effective temperature appreciably higher than that of incandescent lamps [3], but lower than the boiling temperature of the target material. At the same time, the absorption and emission of an individual cluster are resonance in nature. Collective electronic oscillations, the so-called surface plasmons, are excited in clusters upon short-wavelength irradiation. For spherical particles, the resonance takes place for $\omega_s = \omega_p/\sqrt{3} > 3$ eV (where ω_p is the plasma frequency of a macroscopic metal volume [5]), and the resonance effects would be expected to manifest themselves against the emission continuum of the cluster plasma. Naturally, the plasma frequency depends on the electronic structure of the metal. The resonance frequencies of surface plasmons are also affected by the dielectric properties of the environment [5, 6], the particle shape [5, 7], and the degree of aggregation of particles [8]. For instance, when the cluster has the shape of an prolate ellipsoid, the resonance frequency shifts to the red [9]. Note, however, that the resonance peak shape may be distorted by interband transitions [5].

The cluster – radiation interaction efficiency increases when the cluster is part of a fractal structure [10]. A fractal cluster placed in an electromagnetic field may significantly enhance the field strength near the vertices of its branched structure [11]. Due to the large inner surface of a fractal aggregate, the thermal electron emission, which is described by the Richardson model [12], leads to an increase in the electron plasma density in the volume occupied by the fractal. The contribution of the Richardson electrons to the intensity of a continuum spectrum depends on the electronic structure of target atoms via the work function. Note that the electromagnetic field becomes significantly stronger near the vertices of the branched structure of the fractal cluster, increasing the local plasma density due to collisional ionisation. The field emission from the branch vertices according to the Nordheim – Fowler model [13] also leads to the increase in the electron density in the region occupied by the fractal.

It was found [14] that upon evaporation of metals by laser radiation, the number of a group of the periodic table determines the vapour density at which fractal aggregates are most efficiently formed from compact nanoclusters. As the vapour density is increased (for instance, by increasing the external pressure), fractal aggregates unite into a fractal shell [15], which increases the absorptivity and effective brightness temperature of the plasma by limiting the

N.E. Kask, S.V. Michurin, G.M. Fedorov D.V. Skobeltsyn Research Institute of Nuclear Physics, M.V. Lomonosov Moscow State University, Vorob'evy gory, 119992 Moscow, Russia; e-mail: nek@srd.sinp.msu.ru

Received 31 October 2003; revision received 20 February 2004
Kvantovaya Elektronika **34** (6) 524 – 530 (2004)
Translated by E.N. Ragozin

expansion of vapour. Therefore, the electronic structure of target atoms determines, apart from the trite discrete structure of the spectrum, other optical characteristics of the laser plasma as well.

As the density increases, the interaction between the condensate microparticles in the laser plasma becomes stronger to such an extent that the gas plasma transforms to a plasma droplet. As this takes place, the shape and dimensions of the plume change. All this has so far been observed in experiments only for plasmas produced by millisecond pulses when the quasi-stationary evaporation occurs. However, similar effects should take place upon ablation of targets by shorter laser pulses, because the higher the irradiation intensity, the higher the plasma density. Investigations in the nanosecond duration range are complicated by plasma degradation processes and the requirements that the temporal resolution of recording instruments be high enough. We expect that the spectral features of the emission continuum discovered in our work will open up an alternative path for the solution of this problem.

2. Experimental facility and techniques

A pulsed solid-state neodymium-glass laser [16] was used for irradiation. The laser emitted bell-shaped unpolarised 10-ms (FWHM), 1.06-μm pulses with the energy of ~ 100 J. The transverse mode degeneracy in the concentric resonator of the master oscillator ensured the quasi-continuous regime of lasing [17, 18].

Figure 1 shows the scheme of the experimental facility for studying the emission spectra of the laser plume in a wide pressure range (from 0.001 to 100 atm). The target evaporated by laser radiation was placed in a sealed chamber – a steel hollow cylinder with quarts windows and an inner cavity, which measured 25 and 150 mm in diameter and length, respectively. As a buffer gas that determines the external pressure, we used the 99.99 % pure rare gases He, Ar, and Kr.

Polycrystalline metal samples with a purity of 99.9 % and higher served as targets; the surface to be irradiated was subjected to conventional grinding. Control experiments with repeated surface irradiation showed that the quality of surface processing is of no special importance in the range of irradiation duration and intensity used.

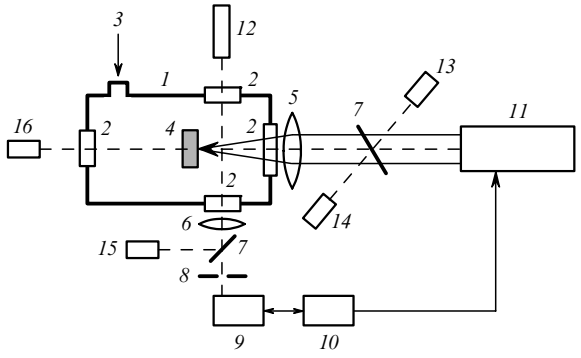

Figure 1. Scheme of the experimental facility: (*1*) chamber; (*2*) quartz windows; (*3*) admission of a buffer gas; (*4*) sample; (*5*) focusing lens; (*6*) condenser lens; (*7*) beamsplitters; (*8*) aperture stop; (*9*) spectrograph with a linear CCD array; (*10*) computer; (*11*) Nd laser; (*12*) He–Ne laser; (*13*, *16*) photomultipliers with 1.06-μm filters; (*14*) photomultiplier with a 0.49-μm filter; (*15*) photomultiplier with a 0.63-μm filter.

The laser radiation propagated along the axis of the experimental chamber and was focused with a spherical lens with a focal distance $F_1 = 300$ mm to a spot of diameter $d \approx 2$ mm on the target surface. We studied the emission spectrum of the plume region located at a distance of about 3 mm from the surface. To eliminate the exposure to radiation from the heated surface, the emission of the plasma region was collected by a spherical quartz lens ($F_2 = 50$ mm) in the direction perpendicular to the axis of the heating laser radiation. The collected radiation was directed via an aperture to the slit of a spectrograph with a 600-lines mm^{-1} diffraction grating.

The spectra were studied in the wavelength range between 0.35 and 1.1 μm with a spectral resolving power of 3900 at 0.589 μm. A two-frame recording of the laser plume emission was made with a CCD linear array (4000 pixels) in the 2000-Å spectral interval during laser pulse irradiation. One frame was processed for ~ 3 ms. An OS-13 colour filter was placed in front of the spectrograph slit to avoid the superposition of diffraction orders. The effective (brightness and colour) plasma temperatures were determined from the intensity ratio between the plume emission and the reference brightness source – an SI8-200U tungsten band lamp, whose emission at a preset current corresponds to the blackbody radiation a with a temperature of 2400 K. To eliminate the effect of the geometrical factor, in the calibration measurements the reference lamp was located in place of the plasma plume.

Note that the plasma absorptivity was estimated from the attenuation of both the heating radiation of the neodymium laser and the He–Ne laser radiation, which passed through the plume in the transverse direction.

3. Emission spectra of the laser plasma at the metal surfaces

Figures 2–6 show the experimental emission spectra of the plasma produced at the surfaces of different metals by laser irradiation with an intensity of 6×10^5 W cm^{-2}. Presented are the results of measurements performed for the $0.42\ \mu m < \lambda < 1.05\ \mu m$ wavelength range for two breakdown regimes – the erosive plume and the bound plasma. Figures 2–4 show the spectra for metals of the I, III, and IV groups of the periodic table, respectively (both main and auxiliary subgroups), Fig. 5 for metals of the VI and VII groups (main subgroups) and Fig. 6 for the transition iron and rare-earth groups.

Upon laser evaporation of any of the metals studied, the continuous spectrum dominates if the bound plasma regime is realised. In the majority of cases this requires rather high pressures (above 30 atm). The atomic spectrum of the corresponding element is observed against the continuous background spectrum as broadened self-reversed atomic absorption lines in the cooled peripheral regions of the plume. On passing to the erosive plume regime, the continuum intensity substantially decreases (by two–three orders of magnitude), atomic emission lines appear in the emission spectrum.

The plasma emission spectra have the following characteristic features:

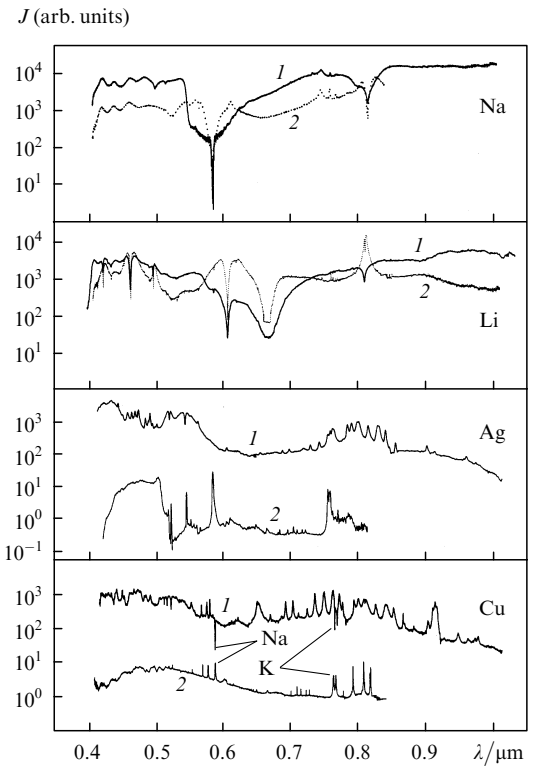

Figure 2. Optical emission spectra for an argon pressure of 30 (*1*) and 1 atm (*2*) for Na, Li, Ag, and Cu.

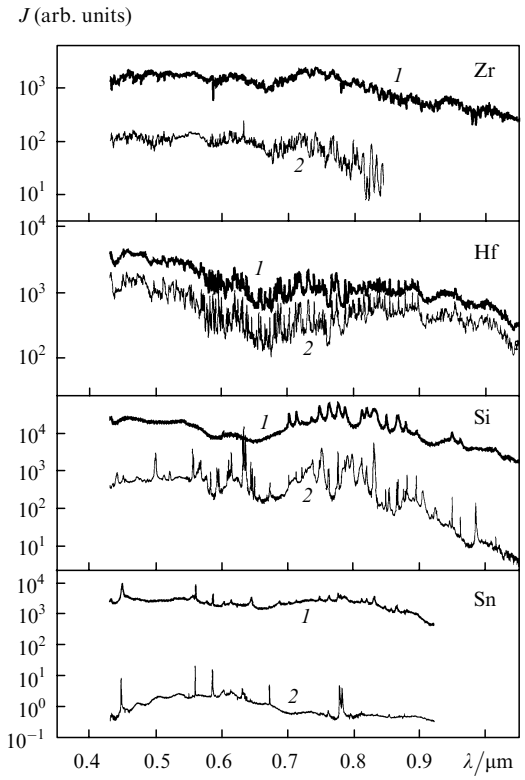

Figure 4. The same as in Fig. 2 for Zr, Hf, Si, and Sn.

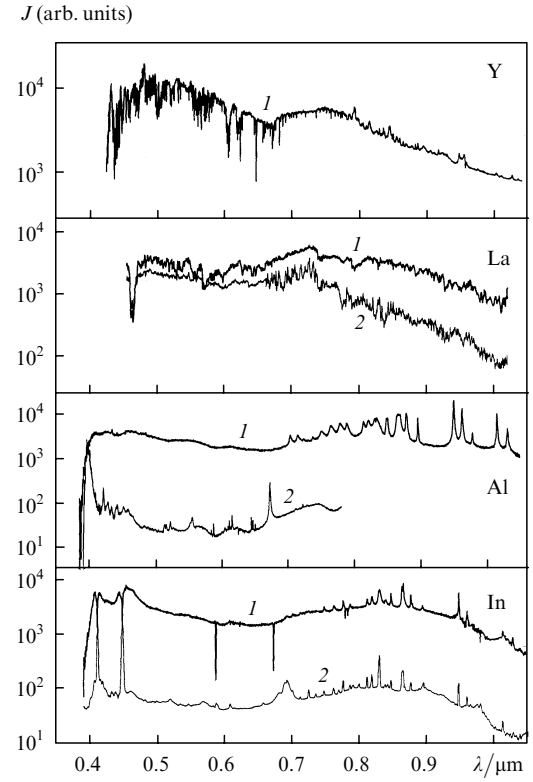

Figure 3. The same as in Fig. 2 for Y, La, Al, and In.

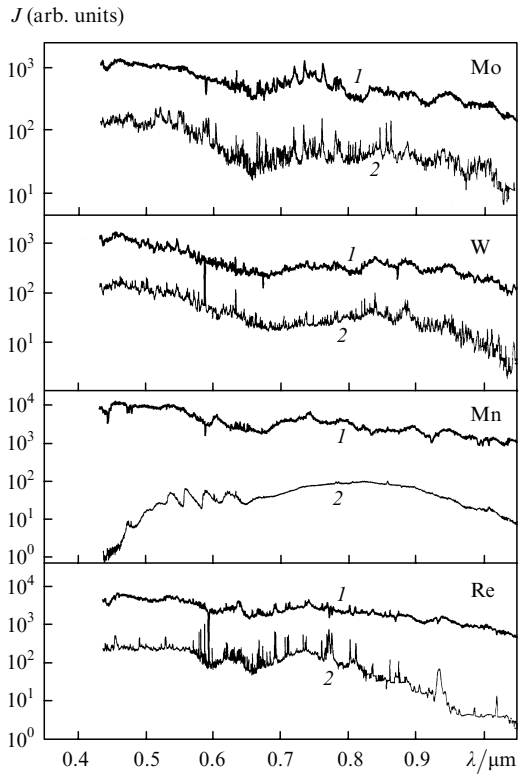

Figure 5. The same as in Fig. 2 for Mo, W, Mn, and Re.

(1) Discrete lines belonging to the ions and molecular compounds of the evaporated material (to dimers, trimers, etc., with the exception of carbon, for which Swan bands are clearly observable) are absent. This indicates that the density of these particles in the irradiation region and, in particular, in the bound plasma is very low. Note that discrete ionic

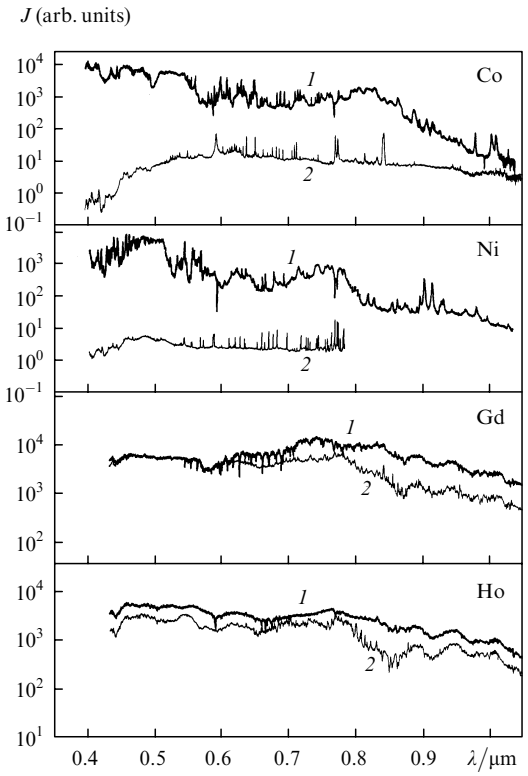

Figure 6. The same as in Fig. 2 for Co, Ni, Gd, and Ho.

lines are reliably recorded at higher intensities of laser radiation (no less than 10^8 W cm^{-2}) [19].

(2) In the bound plasma mode, a line emission spectrum of buffer gas atoms (argon or krypton) is observed against the continuum in the $0.7\ \mu m < \lambda < 0.9\ \mu m$ wavelength range for all investigated elements whose outer shell is made up of s and p electrons. This spectrum is clearly recorded in a relatively narrow pressure range whose boundaries depend on the target material. The data presented in Figs 2–5 were obtained for a pressure of 30 atm, which does not always correspond to the required range. For this reason, the spectrum of a buffer gas observed upon irradiation of the Na, Li, Ca, In, Sn, and Bi metals is seen less clearly than upon irradiation of Mg, Al, Ag, Cu, Si, and Sb. For elements whose outer shell is made up of d and f electrons, this spectrum is absent for any external pressure.

(3) For the elements with d and f electrons in the outer shell, the presence of a large number of narrow atomic lines is typical. As a rule, the emission lines for the elements with d electrons are observed and absorption lines for the elements with f electrons. Because the number of levels for d and f electrons in the energy range below 5 eV is relatively high [20], inelastic losses begin to play a more important role in the energy balance. As a result, free electrons in the laser field cannot gain the energy ($\sim$ 13 eV) required to excite the upper levels of buffer gas atoms. Therefore, the situation in this case is quite similar to that in the breakdown of molecular gases [21, 22]. When the molecular component is present in the laser plasma, which is realised in our experiment, for instance, upon irradiation of metal oxides and fluorides, the discrete spectrum of a buffer gas is not observed, no matter which electrons make up the outer shell of the metal. Therefore, the population of the upper levels (both of the metal atoms and the buffer gas atoms) in the range of light intensities under study is realised not in the course of electron–ion recombination, but as the gas temperature increases, similarly to the situation taking place in an electric arc.

(4) The continuum in the optical spectrum of the laser plume is largely determined by the electron configuration of the outer shell of target atoms. The continuous spectra belonging to some subgroup of the periodic table were observed to be similar. By contrast, a comparison of the spectra obtained upon the evaporation of metals belonging to different subgroups (even though of the same group) reveals significant distinctions. In particular, the ratio between the continuum intensities for different groups (subgroups) significantly changes in going from the normal pressure to 30 atm. For instance, for alkali metals the intensity of continuum only weakly changes, while for the auxiliary subgroup elements (Ag, Cu) it increases by more than two orders of magnitude (see Fig. 2).

(5) Apart from special features inherent in individual subgroups of the elements, the spectra also exhibit common, fairly well-defined features. The spectra corresponding to the bound plasma exhibit a dip in the 0.6–0.8 μm wavelength range, which is most pronounced in the spectrum of Na. The depth of the dip, whose asymmetric profile is plotted in Fig. 2, is determined not only by the vapour density, but by the duration of laser irradiation as well. Evidently, this band appears due to accumulation of the fine-dispersed phase, supposedly compact nanoclusters, in the peripheral plume layers [15].

(6) A characteristic feature of the measured spectra is also the steep slope of the continuum in the IR range. The intensity drop, which is absent in the plasma spectra at the surface of alkali metals, may achieve several orders of magnitude for other elements. The maximum drop is observed for metals of the iron group, for which the continuum intensity in the IR region is two–three orders of magnitude lower than in the blue region (Figs 6a and 6b). Like the broad asymmetric absorption band observed in the sodium vapour, the drop in the IR region can be naturally attributed to the radiation absorption in the cold layers of the laser plume, where nanoparticles are accumulated.

Note that the doublet lines observed in the majority of experiments in the laser plasma spectra correspond to the 3S–3P resonance transitions in the system of atomic levels of the following alkali metals: Na ($\lambda \sim 0.589$ μm), Li (~ 0.671 μm), and K (~ 0.766 μm). Absorption lines are observed in the bound plasma regime and emission lines in the erosive plume regime. In this case, the linewidths are independent of the regime and the external pressure.

4. Effective emission temperature of the laser plasma

Figures 7 and 8 show the results of investigation of the effective plasma emission temperature for laser evaporation of metals respectively at normal argon pressure $p = 1$ atm and a pressure $p = 30$ atm at which the bound plasma regime takes place (an exception was made for Zn and Cd, for which the change of regime occurs at $p \approx 40$ atm). The effective colour plasma temperature was calculated from the frequency dependence of radiation intensity in the short-wavelength spectral region. The blackbody radiation intensity with a temperature of 6000 K varies slightly

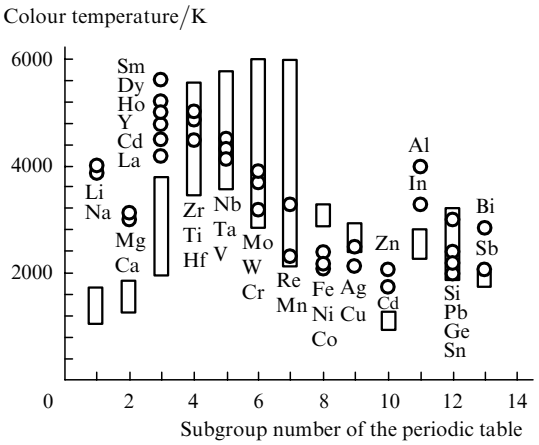

Figure 7. Colour temperature of laser plume radiation for metals from different subgroups of the periodic table at an argon pressure $p = 1$ atm. Empty vertical rectangles specify the range of tabular values of the boiling temperature for the metals investigated.

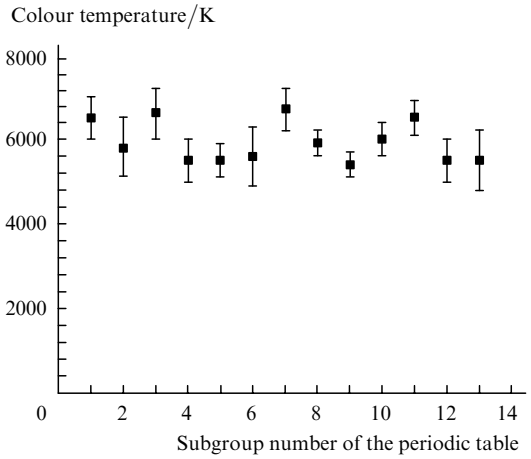

Figure 8. Dependence of the colour temperature on the subgroup number of the periodic table at an argon pressure $p = 30$ atm [for Zn and Cd (10th subgroup), $p = 50$ atm]. The vertical segments correspond to the range of experimental temperature values for different elements of a given subgroup. The relative error of temperature measurements was within 10 %.

throughout the visible wavelength range and is equal to $\sim 6 \times 10^3$ in Figs 2–6.

Figures 7 and 8 show the colour temperature for the investigated metals as a function of the subgroup number of the periodic table, i.e., the so-called long form of the periodic table is used, in which a separate group is allocated to all the elements with the same structure of the outer electron shell [23]. The data presented in Fig. 7 suggest that the subgroup-number dependence inherent in the boiling temperatures of chemical elements is also manifested in the colour temperature of the laser plasma produced near the metal surface at an external pressure of 1 atm.

In the erosive plume regime, the optical thickness of the plasma layer at the frequency of the heating laser radiation is relatively small, and the plasma temperature T would not be expected to differ strongly from the metal boiling temperature T_b. The natural assumption that the inequality $T(p = 1 \text{ atm}) < T_b$ observed for refractory metals (Hf, Zr, Mo, W, and Re) follows from the fact that the absorptivity of the plasma layer is smaller than unity. The absorptivity estimated from the transmittance of the erosive plume is in the range $0.1 < \alpha < 0.3$ and agrees satisfactorily with this assumption. For the majority of metals studied, $T(p = 1 \text{ atm}) \geqslant T_b$, and it is evident that the laser-plasma temperature at their surface is only slightly higher than the temperature of the surface itself. For those elements whose effective temperature is appreciably (by more than a factor of two) higher than the boiling temperature, most likely the erosive plume regime is replaced by the bound plasma regime even at pressures lower than the normal one. This situation is observed for elements belonging to the I–III groups of the periodic table (the main subgroups).

In the bound plasma regime, the radiation absorption in cooled layers is clearly manifested both as reversed lines of atomic spectrum and as broad bands. The latter may be ascribed to either individual compact clusters of the vaporised compound (element) or their aggregates. When these dips are neglected, the emission intensity is well approximated by the blackbody radiation intensity with the effective colour temperature shown in Fig. 8. Note that the colour temperature in the bound plasma regime is close to 6000 K and changes only slightly in going from one element to another. At such a high temperature, all the materials investigated are in the gas phase.

It is commonly assumed [and this situation is evidently realised in electron–ion plasmas produced when the intensity of laser radiation is high enough ($q > 10^7$ W cm^{-2})] that the absorption of laser energy by the plasma in the plume and the intensity of its continuum are determined by free plasma electrons. While free–free transitions are responsible for the radiation with Planck's spectrum, free–bound transitions produce a characteristic step-like structure above the level of this spectrum. The properties of these spectra were calculated in Ref. [24] for free electrons in the cesium plasma with a temperature close to that realised in our experiments for the bound plasma regime. These features are absent in the experimental dependences shown in Figs 2–6. For instance, the recombination continuum should have been ten times stronger than the bremsstrahlung continuum in the short-wavelength region of the laser plasma spectra at the surface of alkali metals (Fig. 2). For Na, the long-wavelength edge of the recombination continuum corresponds to $\lambda_{max} \sim 0.43$ μm. The cause of this discrepancy is evident: in the cluster laser-plume plasma, the decisive part in the absorption and emission of the spectral continuum is played by fine-dispersed particles [3, 4]. When the electron temperature is close to the gas temperature and the temperature of particles, their thermal radiation determines the continuum intensity. This situation is realised in the plasma of the erosive plume.

The effective colour temperature is independent of the target material in the bound plasma regime, which is also typical for the electron temperature at high intensities of laser radiation. We believe that the increase in emission intensity in going over to the bound plasma regime is related to the departure of the electron temperature from the gas temperature. This assumption is required, in particular, to account for the emission of rare-gas atoms observed at high pressures. It is well known that while the threshold of the breakdown of rare gases by neodymium laser radiation is equal to $\sim 10^{10}$ W cm^{-2} [21], it significantly lowers (by two–three orders of magnitude) near the surfaces of metals

and dielectrics [11, 25, 26]. Many experimental and theoretical papers were devoted to the study of this effect. It was found, in particular, that the breakdown arises in separate local microregions [27]. The authors of Ref. [11] showed that 1–2 μm long metallic nibs (microspikes) ~ 0.1 μm in diameter enhance by an order of magnitude the field intensity at their ends and initiate, during their evaporation, the formation of field microregions with a high particle density ($\sim 10^{21}$ cm^{-3}).

It was shown in experiments [14, 15] that nanoparticles accumulated in the peripheral regions of the laser plume. They form upon the dipole–dipole interaction rather long (of the order of several micrometers) filaments, which in turn unite into fractal structures. The field intensity at the ends of the fibres residing in the electromagnetic field may increase by several orders of magnitude. Therefore, the fractal structures accumulated in the laser plume can give rise to a high field intensity in the microregions adjacent to the tips of the branches of these structures and exert effect on the electron temperature, the breakdown threshold, and the character of the emission spectrum. Interestingly, the discrete spectrum of buffer gas atoms which corresponds to transitions from the excited level with an energy of 13 eV is observed only in a relatively narrow pressure range, whose bounds depend on the target material. This range lies above the threshold pressure for the transition to the bound plasma regime and the formation of a fractal shell [14]. On further temperature increase the fractal structure collapses as a result of its melting, which determines the upper bound of the above range.

The electronic structure of atoms is not taken into account as a first approximation, when one considers the emission continuum of a plasma containing a fine-dispersed condensed phase, which arises from the bremsstrahlung and recombination radiation in the interaction of electrons with particles [28]. In this case, the intensity and spectral range of the emission continuum is significantly affected by the radius and charge of the particles. According to Ref. [29], the emission intensity of a laser plume is determined by percolation structures, which precede fractals observed after plasma degradation [14]. The percolation clusters consist of particles with a nanometer dimension R and a charge Z of the order of unity [30]. The characteristic frequency $\{\omega = [Ze^2(mR^3)^{-1}]^{1/2} \sim 5 \times 10^{14}$ s^{-1}, where m is the electron mass$\}$ in the problem on particle-related radiation defines the bound above which the main contribution to the radiation is made by orbital electrons colliding with their mirror images at the particle surface [29, 31]. The calculated value of ω is consistent with the frequency range for which the investigation was carried out. Confirming the validity of this model of emission in a laser plasma invites additional experimental investigation.

5. Conclusions

We have shown in this work that the emission continuum of a laser plume is determined by the electron configuration of the outer shell of target atoms, unlike the thermal radiation of a cluster plasma. In this case, there exists similarity of the optical emission spectra of the laser plume at the surfaces of targets whose atoms belong to the same subgroup of the periodic system. The dependence of the continuum intensity on the external pressure is observed to be similar in character for elements of a common subgroup, which is primarily due to the closeness of the threshold pressures for the plasma transition to the bound state.

Apart from the discrete spectrum of target atoms, broad absorption bands were observed in the continuum spectra, whose shape and position depend on the subgroup number. These bands are adequately interpreted on the basis of a model for the absorption of thermal plasma radiation in cooler peripheral plume regions, in which there occurs accumulation of nanoclusters, micro- and macrofractals observed earlier [14, 15].

The effect of fine-dispersed particles in the plasma manifests itself not only in the absorption of the radiation of central plasma regions, but also in the local enhancement of the heating laser radiation field at the micrononuniformities of fractal structures. As a consequence, there occurs a fictitious lowering of the threshold for rare-gas atom excitation and a discrete emission spectrum appears.

Acknowledgements. This work was supported by the Russian Foundation for Basic Research (Grant Nos 03-02-17026 and NSh-1771.2003.2).

References

1. Gaponov S.V., Luchin V.I., Strikovskii M.D. *Pis'ma Zh. Eksp. Teor. Fiz.*, **6**, 1409 (1980).
2. Zhukhovitskii D.I. *Zh. Eksp. Teor. Fiz.*, **113**, 181 (1998).
3. Smirnov B.M. *Usp. Fiz. Nauk*, **170**, 495 (2000) [*Phys.-Usp.*, **43**, 453 (2000)].
4. Goncharov V.K., Puzyrev M.V. *Kvantovaya Elektron.*, **24**, 329 (1997) [*Quantum Electron.*, **27**, 319 (1997)].
5. Kreibig U., Vollmer M. *Optical Properties of Metal Clusters* (Berlin: Springer, 1995).
6. Hilger A., Cuppers N., Tenfelde M., Kreibig U. *Eur. Phys. J. D*, **10**, 115 (2000).
7. Kottmann J.P., Martin O.J.F. *Phys. Rev. B*, **64**, 235402 (2001).
8. Gartz M., Quinten M. *Appl. Phys. B*, **73**, 327 (2001).
9. Bohren C.F., Huffman D.R. *Absorption and Scattering of Light by Small Particles* (New York: Wiley, 1983).
10. Smirnov B.M. *Usp. Fiz. Nauk*, **163**, 51 (1993).
11. Kovalev A.S., Popov A.M. *Zh. Tekh. Fiz.*, **50**, 333 (1980).
12. Nedospasov A.V. *Usp. Fiz. Nauk*, **94**, 439 (1968).
13. Mesyats G.A., Bychkov Yu.I., Kremnev V.V. *Usp. Fiz. Nauk*, **107**, 201 (1972).
14. Kask N.E., Leksina E.G., Michurin S.V., et al. *Kvantovaya Elektron.*, **32**, 437 (2002) [*Quantum Electron.* **32**, 437 (2002)].
15. Kask N.E., Michurin S.V., Fedorov G.M. *Kvantovaya Elektron.*, **33**, 57 (2003) [*Quantum Electron.*, **33**, 57 (2003)].
16. Kask N.E., Fedorov G.M. *Kvantovaya Elektron.*, **23**, 1033 (1996) [*Quantum Electron.*, **26**, 1007 (1996)].
17. Bonch-Bruevich A.M., Esepkina E.A., Imas Ya.A., et al. *Zh. Tekh. Fiz.*, **36**, 2175 (1966).
18. Aleksandrov V.I., Solov'ev A.G., Ulyakov P.I. *Fizika i Khimiya Obrabotki Materialov*, (4), 30 (1973).
19. Anisimov S.I., Grishina V.G., Dergach O.N., et al. *Kvantovaya Elektron.*, **22**, 815 (1995) [*Quantum Electron.*, **25**, 784 (1995)].
20. Ryabtsev A.N. *Usp. Fiz. Nauk*, **169**, 350 (1999) [*Phys.-Usp.*, **42**, 285 (1999)].
21. Raizer Yu.P. *Osnovy sovremennoi fiziki gazorazryadnykh protsessov* (Fundamentals of the Modern Physics of Gas-Discharge Processes) (Moscow: Nauka, 1980).
22. Vorob'ev V.S., Khomkin A.L. *Fiz. Plazmy*, **10**, 1025 (1984).
23. *Tablitsy fizicheskikh velichin. Spravochnik* (Tables of Physical Quantities. Handbook) I.K. Kikoin (Ed.) (Moscow: Atomizdat, 1976).
24. Baksht F.G., Lapshin V.F. *Pis'ma Zh. Tekh. Fiz.*, **23**, 40 (1997).
25. Bonch-Bruevich A.M., Kaporskii L.N., Romanenkov A.A. *Zh. Tekh. Fiz.*, **43**, 1746 (1973).
26. Barchukov A.I., Bunkin F.V., Konov V.I., Lyubin A.A. *Zh. Eksp. Teor. Fiz.*, **66**, 965 (1974).

27. Bessarab A.V., Zhidkov N.V., Kormer S.B., et al. *Kvantovaya Elektron.*, **5**, 325 (1978) [*Sov. J. Quantum Electron.*, **8**, 188 (1978)].
28. Artem'ev A.A., Yakubov I.T. *Teplofiz. Vys. Temp.*, **28**, 1064 (1990).
29. Kask N.E. *Pis'ma Zh. Eksp. Teor. Fiz.*, **60**, 204 (1994).
30. Kask N.E., Michurin S.V., Fedorov G.M. *Teplofiz. Vys. Temp.*, **37**, 9 (1999).
31. Fortov V.E., Yakubov I.T. *Neideal'naya plazma* (Nonideal Plasmas) (Moscow: Energoatomizdat, 1994).